Towards Parallel Quantum Computing for Industrially Relevant PDEs

Quantum remeshing VQA implementation for heat equation

|Ulysse Remond⟩ |Pierre-Emmanuel Emeriau⟩ |Joseph Mikael⟩ |Samuel Donachie⟩
|Arthur Mathorel⟩ |Riccardo Mengoni⟩ |Kyryl Kazymyrenko⟩

October ???



EDF Weling QUANDELA

Towards Parallel Quantum Computing for Industrially Relevant PDEs

Quantum remeshing VQA implementation for heat equation

Cyril Kazymyrenko (EDF)

AQADOC, October 15, 2026



eDF Welinq QUANDELA

Outline

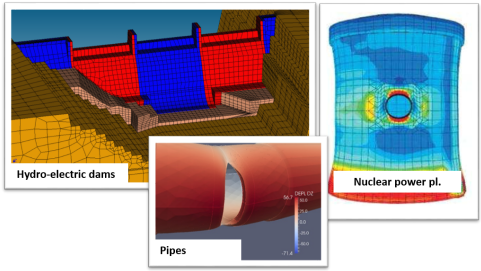
1. Motivation
2. Stiffness matrix encoding
3. VQA with Quantum Remeshing
4. Parallel Quantum Computing perspectives

Relevance of PDE Solutions

- Numerical solution of **Partial Differential Equations (PDEs)** is central to the design, monitoring and safety assessment of large industrial infrastructures.
- Representative applications:
  - Dams and hydraulic structures
  - Pipelines and fluid transport
  - Buildings and civil engineering
- Typical finite-element simulations: 10^6 degrees of freedom (DoFs)
- Long-term industrial targets size: $\sim (100m)^3/1mm^3 \Longrightarrow$ $\mathbf{10^{15}}$DoFs

Most industrial models are **nonlinear**:

- Damage, Fracture, Plasticity
- Hydraulic flows



Dams, pipes, structures and energy systems

State of the art of Quantum PDE Solvers

Physical World

Nonlinear PDEs



$\partial_t u = \mathcal{N}(u, \partial u)$

$\Longrightarrow$

Kolmogorov (1931)
Carleman (1932)

Quantum Computer

Linear Evolution



$|\psi\rangle \to U|\psi\rangle$ or
$Ax = b$

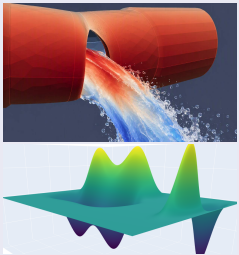
$\Longleftrightarrow$

VQLS (2019)

$\Longleftrightarrow$

Classical Computer

NL Optimization



$|\psi(\theta)\rangle \to \min_\theta C(\theta)$

Quantum PDE solvers bridge the nonlinear physical world to the nonlinear optimization.

From Industrial PDEs to Quantum Linear Solvers

Industrial PDE Test Cases

$$\mathbf{Ax} = \mathbf{b}, \qquad A \in \mathbb{R}^{N \times N}$$

Examples:

- Heat transfer
- Fluid flow
- Linear elasticity
- Fracture mechanics

Computational challenge

- Large sparse matrices
- Typical meshes: $N \sim 10^6 - 10^9$ DoFs

Variational Quantum Linear Solver (VQLS)

$$\min_{\theta} \| A|x(\theta)\rangle - |b\rangle \|^2$$

- NISQ compatible
- Not scalable

Quantum Singular Value Transformation (QSVT)

$$A^{-1} \approx poly(A)$$

- Best asymptotic scaling
- Fault-tolerant perspective
- Requires block encoding

Classical versus Quantum Scaling for sparse $Ax = b$

Classical CG

$$\mathcal{O}\left(N\sqrt{\kappa}\log\frac{1}{\varepsilon}\right)$$

Memory:

$$\mathcal{O}(N)$$

Quantum QSVT

$$\mathcal{O}\left(\kappa \log N \log\frac{\kappa}{\varepsilon}\right)$$

Memory:

$$\mathcal{O}(\log N)$$

where

$N =$ number of DoFs, $\quad \kappa = \mathrm{cond}(A)$, $\quad \varepsilon =$ target accuracy, $\quad d =$ dimension.

For elliptic PDEs : $\kappa \sim N^{2/d} \Longrightarrow$ The advantage is **polynomial** (not exponential) in runtime, but **exponential** in memory compression

Target PDEs

Heat Transfer (Poisson Equation)

$$-\nabla \cdot (k \nabla T) = f$$

Linear Elasticity (Navier–Cauchy)

$$\mu \Delta u + (\lambda + \mu) \nabla (\nabla \cdot u) = 0$$

Quantum challenges

$$f \longrightarrow |f\rangle \qquad |u\rangle \longrightarrow u(x = 0)$$

boundary encoding observable extraction

Stationary THM System

$$\begin{cases} -\nabla \cdot (k_T \nabla T) = f_T, \\ -\nabla \cdot (k_p \nabla p) = f_p, \\ -\nabla \cdot (\mathbb{C} : \varepsilon(u) - \alpha_B p I - \beta_T T I) = 0. \end{cases}$$

Unknowns

- T: temperature field
- p: pore pressure field
- $u = (u_x, u_y, u_z)$: displacement field

Quantum-Friendly 2D Heat Equation

Screened Poisson Equation

$$-\Delta T + \beta T = f; \qquad \text{Domain } \Omega = [0, L]^2$$

with periodic boundary conditions.

After finite-difference (FD) discretization:

$$A = (2I - S - S^\dagger) \otimes I + I \otimes (2I - S - S^\dagger) + \beta I$$

where S is the unitary shift operator:

$$S|i\rangle = |i + 1 \bmod N\rangle.$$

Advantages

- Direct LCU decomposition:

$$A = \sum_{j=0}^{4} \alpha_j U_j, \text{ with } U_j = I \otimes S$$

- in QSVT: 3 ancilla qubits.
- in VQA: 3 measures.

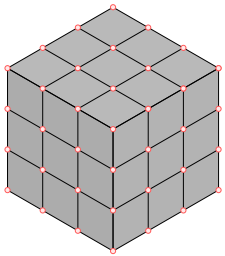
Limitations

- Only volumetric source f.
- Requires regularization $\beta \neq 0$.

3D Heat Equation Benchmark

S. Donachie et al., arXiv:2510.15645 (2025).

$$-\Delta T = f; \qquad \text{Domain } \Omega = [0, L]^3$$



- Neumann and Dirichlet conditions.
- Finite Elements Discretization:

$$A = \sum_{abc=0}^{63} \alpha_{abc} U_a \otimes U_b \otimes U_c.$$

- A - structured operator of tensor-products $(I, S) \Rightarrow (I, \mathbb{D}, \mathbb{T}, \mathbb{U})$

$$\mathbb{D} = \begin{pmatrix} 1 & \dots & 0 & 0 \\ \vdots & \ddots & \vdots & \vdots \\ 0 & \dots & 1 & 0 \\ 0 & \dots & 0 & 0 \end{pmatrix}; \qquad \mathbb{T} = \begin{pmatrix} 0 & 1 & \dots & 0 \\ \vdots & \ddots & \ddots & \vdots \\ 0 & 0 & \ddots & 1 \\ 0 & 0 & \dots & 0 \end{pmatrix};$$

2D Navier–Cauchy Benchmark

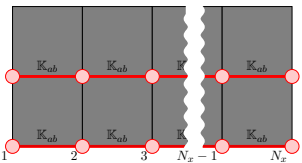
U. Rémond et al., arXiv:2510.14746 (2025).

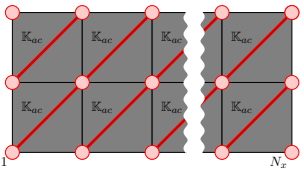
$$\mathrm{grad}(\mathrm{div}\, u) + (1 - 2\nu)\Delta u = 0, \qquad u = (u_x, u_y)$$

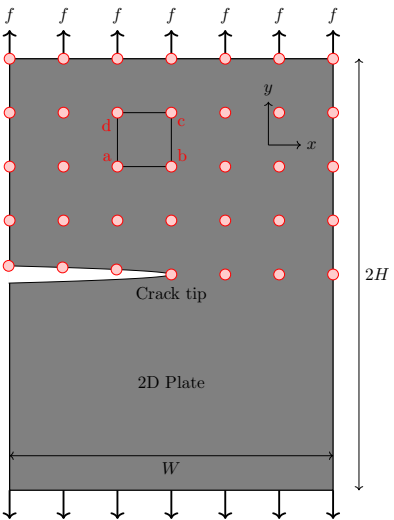
- Rectangular domain with central crack

The decomposition of A with help of $\mathbb{D}_{N_y} \in \mathbb{R}^{N_y \times N_y}$, $\mathbb{T}_{N_x} \in \mathbb{R}^{N_x \times N_x}$ and the elementary stiffness matrix $\mathbb{K}_{ij} \in \mathbb{R}^{2\times 2}$:

$$A = \mathbb{D}_{N_y} \otimes \mathbb{T}_{N_x} \otimes \mathbb{K}_{ab} + \mathbb{T}_{N_y} \otimes \mathbb{T}_{N_x} \otimes \mathbb{K}_{ac} + \cdots .$$







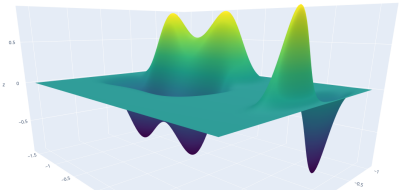
Increasing Physical Complexity

Small-scale QPU benchmark

- Mixed Boundary Conditions
- Finite Elements Discretization

Consequences

- No unitary separability
- Harder quantum encoding



QSVT

$\Longrightarrow$

VQA ?

QSVT

- Non trivial Block encoding
- Extra memory: ancilla qubits
- Deep quantum circuit

VQA

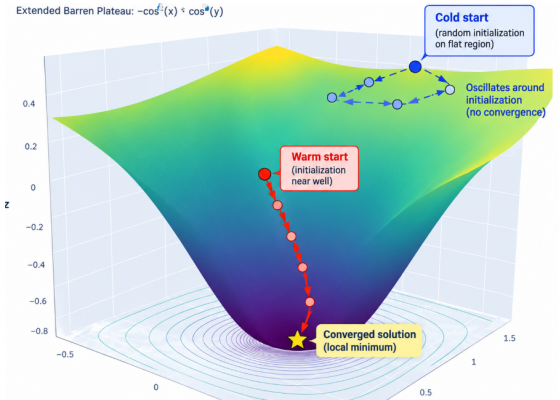
- Barren plateaus
- Difficult optimization
- No size-scaling

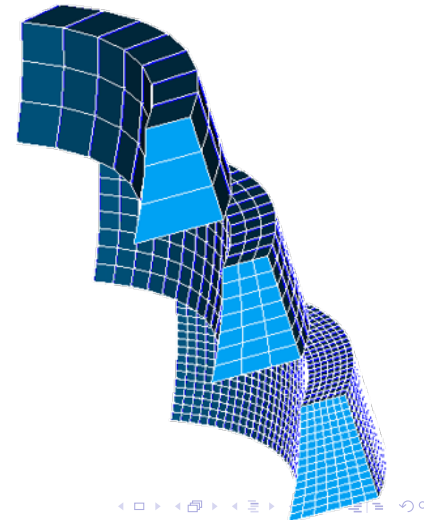
Quantum Remeshing Concept

Coarse solve $\rightarrow$ Mesh refinement $\rightarrow$ State transfer $\rightarrow$ Fine-scale optimization

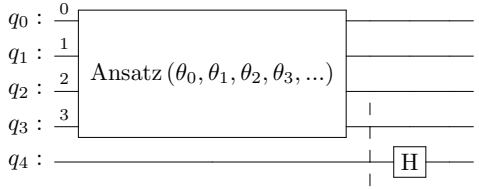
$$N_x \rightarrow 2N_x \rightarrow 4N_x \rightarrow \cdots$$

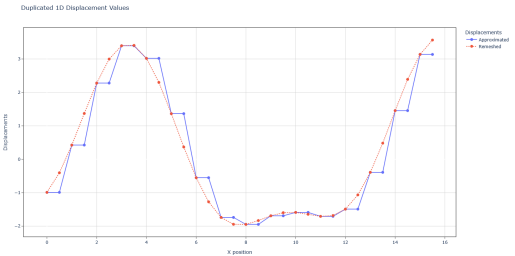
Goal: Mitigate barren plateaus.

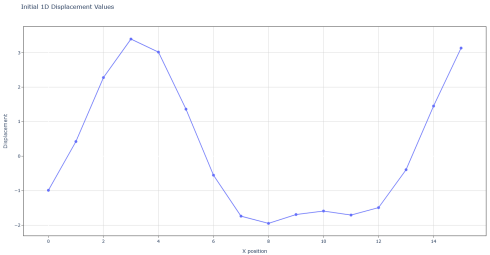


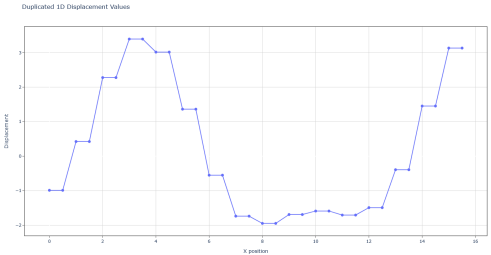


Quantum Remeshing in 1D





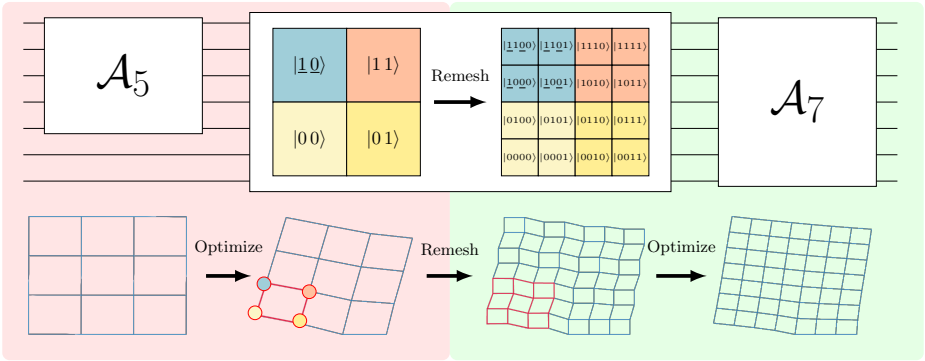




[1]PhD Ulysse Rémond

VQA Workflow in 2D

$|0\rangle \rightarrow$ Coarse VQA $\rightarrow$ Remeshing $\rightarrow$ Fine VQA $\rightarrow |x\rangle$

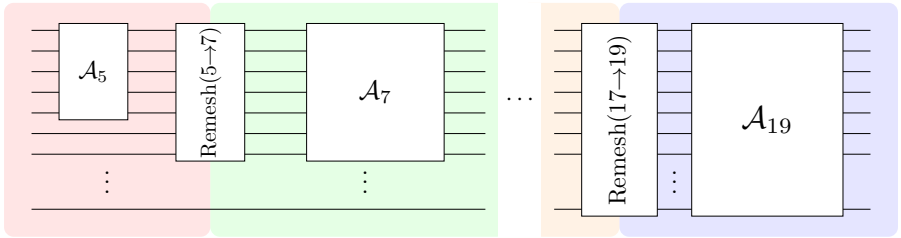


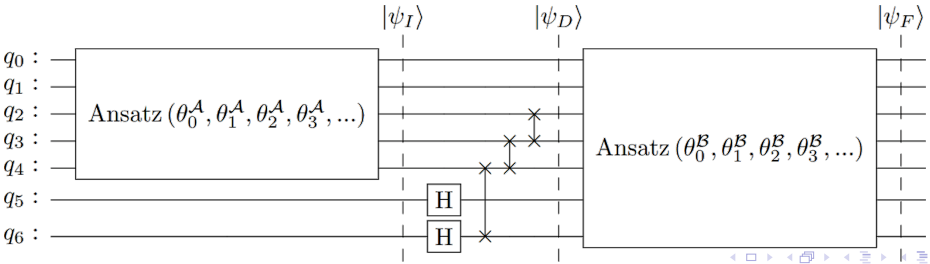
Two additional qubits - one in each spatial direction [2]

[2] see PhD Ulysse Rémond

Cascade remeshing: 2D or 3D

for r in range(5): $|x\rangle_r \rightarrow$ Coarse VQA $\rightarrow$ Remeshing $\rightarrow$ Fine VQA $\rightarrow |x\rangle_{r+1}$

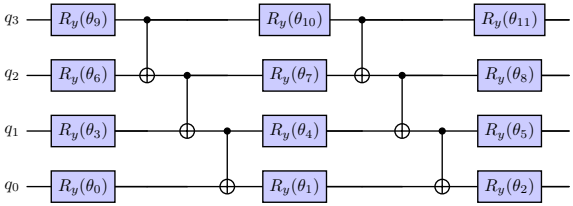




3D Heat: Convergence failure for the random "cold start"

Cost function from (Sato et al 2021)

$$C(\psi(\theta)) = -\frac{1}{8}\frac{\left(\langle\psi(\theta)|b\rangle + \langle b|\psi(\theta)\rangle\right)^2}{\langle\psi(\theta)|\,A\,|\psi(\theta)\rangle}$$



Accuracy convergence issue due to Barren plateaus

VQA performance with random cold starts (averaged over 100 2h-optimization runs).
RY-CNOT (qiskit *RealAmplitudes*): initial accuracy 0%, target accuracy 100%

Qubits	Par	Mean Cost (%)	NEWUOA Iterations	Max Cost (%)
9	108	23.6 ± 2.4	4106 ± 1308	29.4
12	252	4.0 ± 0.7	4625 ± 2965	5.3
15	330	0.53 ± 0.03	4867 ± 796	0.57

see Donachie et al. arxiv/2510.15645

3D Heat: cascaded remeshing and IonQ QPU execution

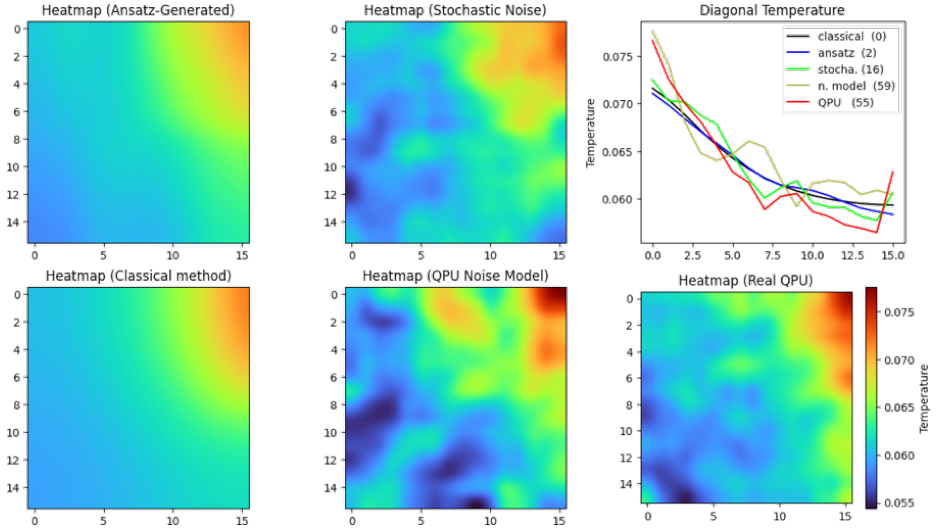
State-vector: Improvement of initialization strategies for different ansätze, 15 qubits system

Ansatz	Cold Start	Uniform Guess	Cascade Warm-Start
RY-CNOT	$0.53 \pm 0.03\%$	$54.71 \pm 5.02\%$	$62.5 \pm 4.84\%$
RX-RY-CNOT	$0.21 \pm 0.04\%$	$46.7 \pm 2.90\%$	$72.1 \pm 1.45\%$

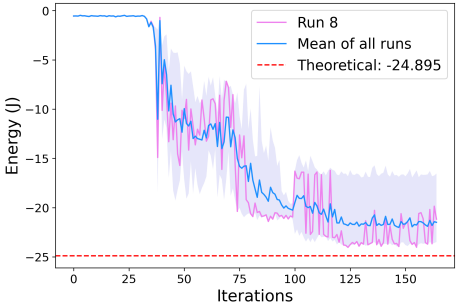
QPU runs on IonQ: Comparison of ideal, noisy simulation, and QPU results.

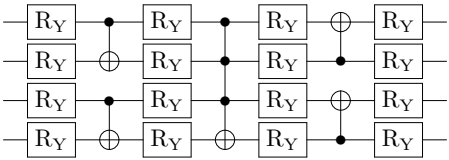
Qubits	Ideal	Noisy Simulation (100k shots)	QPU (10k shots)
6	97.1%	93.5%	92.2%
9	94.4%	80.2%	–
12	92.2%	20%	–
15	74.0%	2%	–

Separate 2D Heat benchmark: 8 qubits QPU execution on IonQ



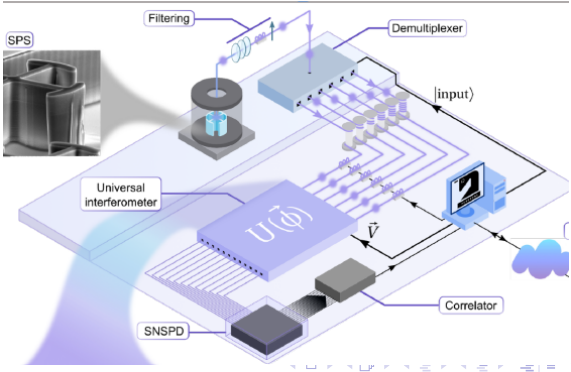
Crack benchmark: 4 qubits QPU on photonic Quandela computer





see U. Rémond et al., arXiv:2510.14746.

- Tailored test: QLOQ ansatz, $u > 0$, etc
- Full VQA execution
- 10 different runs
- 96.6% accuracy



What Next? Towards Parallel Quantum Computing

Single quantum processor

Accessible problem sizes

- Statevector simulation $\sim 10^6$ DoFs
- Noisy simulation $\sim 10^3 - 10^4$ DoFs
- **Real QPU** $\sim 10^2 - 10^3$ DoFs

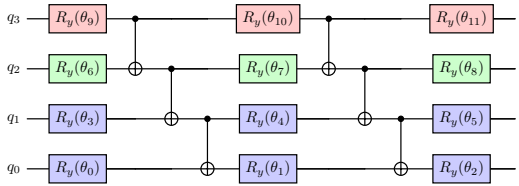
Key ingredient

- Variational quantum linear solvers
- Progressive refinement of the solution
- Industrially relevant PDE test cases

Open Question

How can we go beyond a single QPU?

Quantum remeshing



Progressive activation of fitting parameters:
Blue (2 qubits)⇒ Green (3 qbs)⇒ Red (4 qbs)

Parallel Quantum Computing

$$QPU_1 \leftrightarrow QPU_2 \leftrightarrow QPU_3$$

Multiple weakly coupled QPUs

Parallel Quantum Computing

Multiple quantum processor

Accessible problem sizes

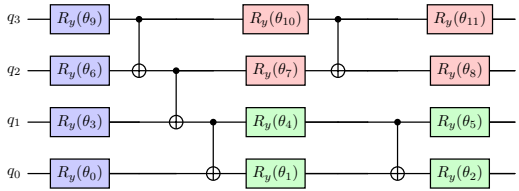
- Statevector simulation $\sim 10^6$ DoFs
- Noisy simulation $\sim 10^3 - 10^4$ DoFs
- **Real QPU** can reach $\sim 10^4$ DoFs?

2D screened Poisson Equation

$$-\Delta T + \beta T = f; \qquad \text{Domain } \Omega = [0, L]^2$$

$$T(x, y) \approx \sum_{i=1}^{k} \alpha_i \, f_i(x) \, g_i(y), \quad k \ll N$$

Entanglement control via Blue gates



Fitting parameters roles:

Red (x-dependence) $\Leftrightarrow$ Red (y-dependence)

Parallel Quantum Computing

$$QPU_1 \leftrightarrow QPU_2$$

Two single CNOT coupled QPUs

Perspectives

Short term

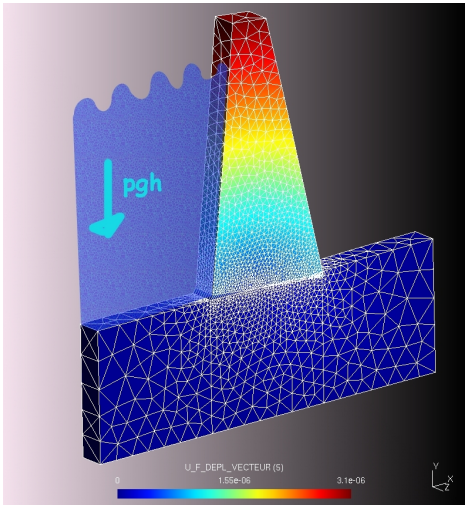
- Two QPUs 2D VQA
- Filtering of singular solutions
- Hardware benchmarks

Mid term

- 3D VQA extension
- Adaptation for QSVT
- Optimized block encoding

Long term

Coupled thermo-hydro-mechanical simulations for crack propagation and dam safety.

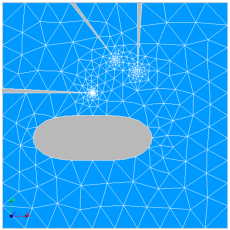


The End

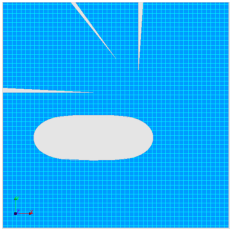
First step to quantum advantage



Multi-crack problem



Classical mesh

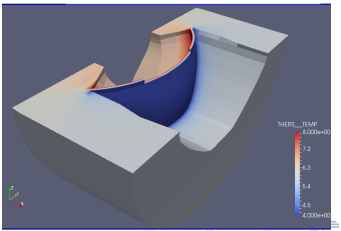


Quantum mesh

Two possible benchmarks

- Multiple crack propagation in solid mechanics.
- Coupled thermo-hydro-mechanical (THM) problem.
- Long-term objective: THM of concrete dams.

  Heat $\leftrightarrow$ Flow $\leftrightarrow$ Mechanics $\Longrightarrow$ Cracks in dams

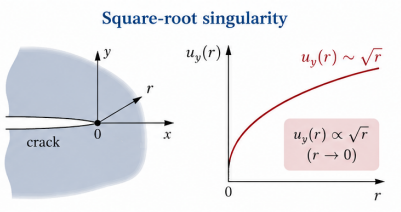


Relevant observables in linear mechanics

Solution singularity:
N. I. Muskhelishvili (1932,1942)

$$u_y(r) \approx \text{SIF} * 2(1-\nu^2)\sqrt{2r/\pi}, \quad \text{for } r \approx 0$$

Stress intensity factor (SIF): characterizes the amplitude of the near-tip singular field



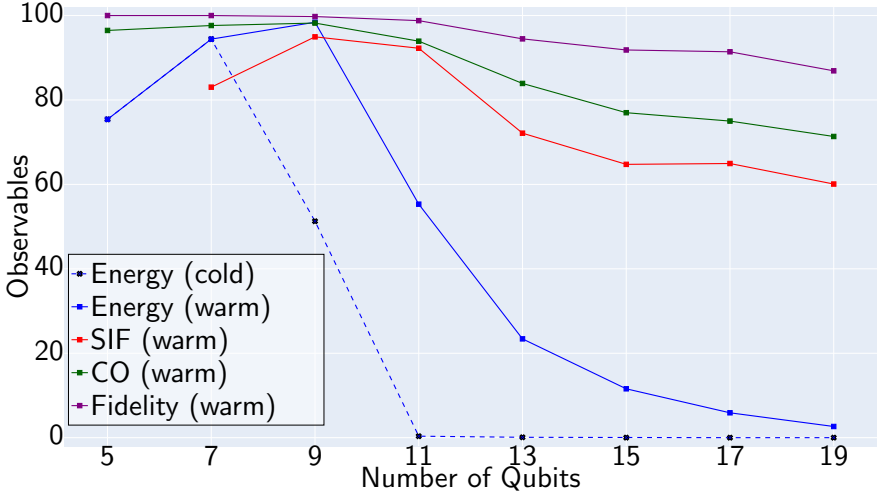
Quantum SIF (QSIF): function of observables

$$\text{QSIF} \sim ||u|| \sqrt{\int [u_y(x,0)]^2 \, dx} = ||u|| \sqrt{\langle \psi | \mathbb{P} | \psi \rangle}$$

if QSIF$> 1 \Rightarrow$ crack propagation

- $u_y(x,0)$: crack-opening displacement (COD).
- $||u||$: state normalization.
- $\mathbb{P}$: projector onto the crack-opening degrees of freedom.
- $\langle \psi | \mathbb{P} | \psi \rangle$: expectation value of $\mathbb{P}$.

Crack benchmark: convergence of mechanical observables

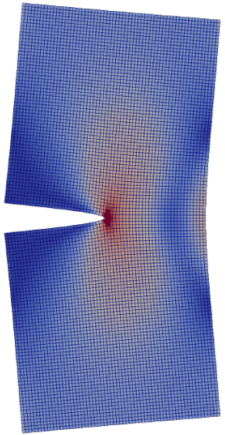


Cascaded simulations from 5 to 19 qubits

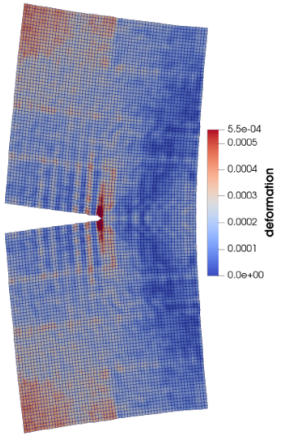
48h optimization at each step

50% precision of observables COD and SIF.

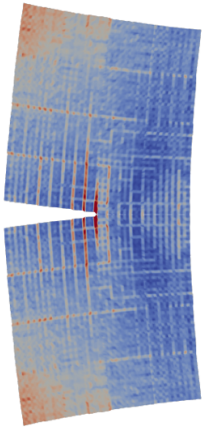
Crack benchmark: ghost grid, as remeshing artifacts



(a) The deformation map discretized using 2^{13} DoF, generated by Code_Aster.



(b) The 13 qubits cascaded quantum solution with the 90% convergence in COD.



(c) The 15 qubits next step remeshing. The field relaxation error increases.